International Journal of Advances in Engineering and Management (IJAEM)
Volume 7, Issue 11 Nov. 2025, pp: 280-296 www.ijaem.net ISSN: 2395-5252

Unsteady MHD Quadrative Thermal Radiative Flow of Carreau Fluid along a Stretching Cylinder with Heat Generation

Isaac Oluyemi Onikola[1], Olusegun Adebayo Ajala[1],Peter Adegbite[1,] Akintayo Oladimeji Akindele[1] Sunday Oloruntoyin Sangoniyi[2], Azeez Ajani Waheed[3]

[1]Department of Pure and Applied Mathematics, Ladoke Akintola University of Technology, Ogbomoso, Oyo State, Nigeria
[2]Department of Mathematics, Emmanuel Alayande University of Education, Oyo, Oyo State, Nigeria
[3]Department of Mathematics, Lead City University, Ibadan, Oyo State, Nigeria

---

Date of Submission: 15-11-2025 Date of Acceptance: 25-11-2025

ABSTRACT
A two-dimensional unsteady flow of an incompressible and electrically conducting Carreau fluid along a stretching cylinder with incorporation of heat generation, quadratic thermal radiation and magnetic field is considered. The set of partial differential equations formulated is transformed to system of non-linear ordinary differential equations using adequate similarity transformation variables. Numerical solutions to the resultant non-dimensional equations are computed using the Runge-Kutta fourth order method alongside shooting technique which is implemented on Maple 18.0 software. The numerical results are examined for the emerging parameters and the behavior of flow parameters on velocity and temperature distribution profiles of the fluid are sketched and analyzed physically. The results indicate that the velocity profile of the fluid reflects an initial decrease which later switches over to increase velocity with an increase in unsteadiness parameter while the fluid velocity is enhanced with an increase in Weissenberg number and curvature parameter but decreases by escalating the magnetic field and melting parameter. The fluid temperature increases as thermal radiation parameter, temperature ratio parameter due to large temperature difference. Also, the thermal boundary layer is boosted with an increase in heat generation and unsteadiness parameters but decays when there is a rise in the Prandtl number and melting parameter. The findings drawn from this analysis are applicable in many areas, including heat exchangers in electronics, space cooling, power generation, magnetic drug targeting and automotive engineering.

Keywords: Carreau fluid, Quadratic thermal radiation, Heat generation, Unsteady flow, Melting heat transfer.

Nomenclature

x	Axial coordinate of the cylinder
r	Radial coordinate perpendicular to the cylinder axis
u	Fluidvelocity along x - direction
v	Fluidvelocity along r - direction
ρ	Fluid density
υ	Fluid kinematic viscosity
B_0	Magnetic induction
k	Thermal conductivity of the fluid
σ^*	Stefan-Boltzmann constant
σ	Electrical conductivity of the fluid
k^*	Mean absorption coefficient
c_p	Specific heat capacity
q_r	Radiative heat flux
c_s	Heat capacity of the solid surface
a	Characteristics length
λ_1	Latent heat of the fluid of the melting layer
U_w	Stretching surface velocity
U_∞	Ambient fluid velocity
U_0	Reference stretching velocity

International Journal of Advances in Engineering and Management (IJAEM)
Volume 7, Issue 11 Nov. 2025, pp: 280-296 www.ijaem.net ISSN: 2395-5252

T_w Temperature of the melting surface of the cylinder
T_0 Temperature of the solid surface
T_∞ Ambient fluid temperature
η Dimensionless similarity variable
Q_0 Uniform volumetric heat generation constant
Γ Relaxation time constant
n Power law index
A unsteadiness parameter
Rd Thermal radiation parameter
θ_w Quadratic thermal radiation
δ Heat generation parameter
λ Curvature parameter
Me Melting parameter
We Weissenberg number
M Magnetic field parameter
Pr Prandtl number
D(f)(η)Differentiation with respect to η

Subscripts
w Stretching surface condition
0 Fluid reference condition
∞ Fluid ambient condition

Superscripts
$'$ Differentiation with respect to η

Acronyms
MHD Magneto hydrodynamics
PDE Partial Differential Equations
ODE Ordinary Differential Equations

I. INTRODUCTION

The study of heat transfer along a stretching cylinder has gained considerable interest of many researchers due to its application in many areas of engineering and applied physics. The creation, utilization, conversion, and exchange of thermal energy between physical systems are the focus of the thermal engineering field of heat transfer. Convection, thermal radiation, heat conduction, and energy transfer via phase transitions are some of the various mechanisms that make up heat transfer. Thermal equilibrium occurs when an object's temperature differs from that of another object or area around it and heat moves between them until they both achieve the same temperature. In accordance with the second rule of thermodynamics, this natural heat transfer often takes place from one area of high temperature to another area of low temperature [1]. Gnaneswara [2] examined the analysis of modified Fourier law and melting heat transfer in a flow involving carbon nanotubes. The result revealed that velocity and corresponding thickness of the boundary layer declined for rising values of Forchheimer parameter and porosity parameter.

Imran et al.[3] studied the impact of Joule heating and melting on time-dependent flow of nanoparticles due to an oscillatory stretchable curved wall. It was observed that the Nusselt number was raised by the melting effect and the reverse tendency happened for the Joule heating. The impact of the irregular chemical reaction, heat generation and melting heat transfer on a stagnation point micropolar fluid over a flat plate via stretchable surface was examined by Singh et al.[4]. Muhammad et al.[5] looked into numerical research for melting heat in hybrid nanofluid dissipative flow on a variable thicked surface. It was shown that the hybrid nanofluid functioned better when melting heat transfer and viscous dissipation were present. Khan [6]used irreversibility analysis to investigate melting heat transmission in radiative flow of nanomaterials. The outcome demonstrated that while a greater melting parameter reduced the temperature distribution, a higher melting rate increased the velocity field.

Gireesha et al.[7] used the Cattaneo-Christov heat flux model to study the melting heat transfer and magnetohydrodynamic flow of a dusty Casson fluid across a stretching sheet. The dusty phase temperature is lowered by melting heat transfer, according to the numerical data. Ayub et al. [8] used the Keller-Box and BVP4C approach to study the properties of melting heat transport of blood using a time-dependent cross-nanofluid model. The blood was represented by the cross-fluid model, which had a favorable impact on the melting heat transfer. Jawad et al. [9] investigated the analysis of hybrid nanofluid stagnation point flow with melting heat transfer over a stretching surface. According to the analysis, the velocity profile increased as the electric field and slip parameter increased while the magnetic field decreased.

The thermal radiation effect has major implications in science and technology which has piqued the interest of many researchers. This encompasses nuclear reactor cooling, power generation, combustion, space vehicles, space technologies, and high-temperature procedures. Warke et al.[10] examinednumerical investigation of the stagnation point flow of radiative magnetomicropolar liquid past a heated porous stretching sheet. Ajala et al. [11] studied the effects of thermal radiation and convective heating on nanofluid hydromagnetic boundary layer flow past a stretchable permeable surface. It was concluded that increasing the solid volume parameter, Hartman number and suction parameter resulted in a drop in momentum boundary layer thickness, but an increase in permeability. Thriveni and Mahanthesh [12] investigated heat transfer of a hybrid nanomaterial in an annulus using the quadratic Boussinesq approximation.Ajala et al. [13] evaluated the bio-convection flow of micropolar nanofluids across an inclined permeable stretching surface with radiative activation energy.

Rosseland linear thermal radiation assumes a modest temperature difference, whereas quadratic thermal radiation modelling takes into account a large temperature difference. To address this disparity, Thriveni and Mahanthesh [14] presented a new dimension that incorporates the Rosseland thermal radiation aspect when quadratic thermal convection is considered in their model. The series after the quadratic term was truncated rather than the series after the linear term. This phenomenon is known as Rosseland quadratic thermal radiation. As a result of the small temperature differential, the conventionally linear Rosseland approximation is no longer appropriate. Hence, the utilisation of quadratic Rosseland thermal radiation with large temperature differences is taken into consideration and desired for manufacturing processes. Algehyne[15] examined mixed convective flow of Casson and Oldroyd-B fluids through a stratified stretching sheet with nonlinear thermal radiation and chemical reaction. Entropy generation analysis from the time-dependent quadratic combined convective flow with multiple diffusions and nonlinear thermal radiation was investigated by Patil and Goudar[16]. Shaw et al. [17] examined hydromagnetic flow and thermal interpretations of Cross hybrid nanofluid influenced by linear, nonlinear and quadratic thermal radiations for any Prandtl number.

Carreau [18] developed the Carreau fluid model in 1972 to accurately characterise non-Newtonian viscous fluids. Carreau's proposed constitutive model is known as a generalised non-Newtonian fluid model that has four more parameters than the Newtonian case. The model is commonly used in the study and development of medicinal compounds, polymeric suspensions, food processing, lubrication issues, blood and chemical combustion.Santoshi et al.[19] examined numerical scrutinization of three dimensional Casson-Carreau nanofluid flow. Mahdy et al. [20] studied the usefulness of activation energy in dusty Carreau fluid flow over a stretching cylinder due to varying thermal conductivity and a temperature-dependent heat source/sink. The heat flow decreased as the dust particle's mass concentration increased. Afzal et al. [21] studied the importance of unsteady double diffusion on Carreau micropolar nanofluid movement across an expanding sheet with thermo-radiation and a uniform heat source, employing the RK-4 algorithm and the shooting method. Fateh et al. [22] investigated the role of a quadratic-linearly radiating heat source in Carreau nanofluid with exponential space-dependent behaviour via a cone and wedge.

Unsteady heat and mass transfer mechanisms in MHD Carreau nanofluid flow were investigated by Khan et al. [23]. It was determined that while the local Sherwood number and Nusselt number fell as the thermophoresis parameter increased, the dimensionless temperature and nanoparticle concentration increased in the presence of a magnetic field. Gangadhar et al. [24] used the spectrum relaxation approach to investigate the MHD flow of a Carreau fluid past a stretching cylinder with Cattaneo-Christov heat flux. A novel modeling approach for 3D Carreau fluid flow that takes nonlinear thermal radiation into account was examined by Khan et al. [25]. As seen by the velocity profiles, the Weissenberg number (We) for the shear thinning and shear thickening liquids exhibited contradictory behavior. Al-Azawy et al. (2020) investigated both Newtonian and non-Newtonian blood rheology in a stenosis model. When the Carreau and Newtonian models were examined, it was found that the non-Newtonian model levels were expected to be higher in the 90% blockage than in the 70%. The performance of the second law in Carreau fluid flow via an inclined microchannel under radiative heated convective conditions was examined by Madhu et al. [26]. Chu et al. [27] used dual simulations utilizing the Runge-Kutta Fehlberg technique to study mass and heat transfer in hydromagnetic stagnation point flow of Carreau nanomaterial.

In a more recent study, Yeouet al. [28] examined the quadratic thermal radiative effects on Carreau fluid through a melting stretching cylinder. It was revealed that the melting phenomena reduced the velocity and temperature profiles, indicating that increasing the melting parameter improved the mobility of fluid particles. Additionally, the quadratic effect of thermal radiation raised the local Nusselt number.Maqbool et al. [29] examined mixed convective heat and mass transfer of Carreau fluid flow past over a permeable stretching disk: thermal and concentration analysis. Thermal investigation of the melting influence on the flow of Carreau fluid around a stretchable cylinder with quadratic radiation was examined by Lim et al. [30].Onikolaet al. [31] investigated Magnetohydrodynamic Flow of Carreau Fluid over a Stretching Cylinder with Quadratic Thermal. It was discovered that the fluid temperature enhanced as the thermal radiation and temperature ratio parameter due to quadratic thermal radiationboosted. Sarma, Dipak, and Mudoi[32] studied electromagnetohydrodynamic flow and impact of Soret, Dufour, Hall current, and activation energy on Carreau fluid through a stretching cylinder.Song [33] examined aspects of thermal diffusivity and melting phenomenon in Carreau nanofluid flow confined by nonlinear stretching cylinder with convective Marangoni boundary constraints. The outcomes yielded that presence of melting parameter and Weissenberg number improved the nanofluid velocity.

Despite the aforementioned, no study has examined the thermal behavior of Carreau fluid flow along a stretching cylinder when unsteadiness, heat source, quadratic thermal radiation and magnetic field are all present. As a result, this work improves on earlier research by Yeouet al. [28] and Song et al. [33] by investigating the quadratic thermal radiative effect on Carreau fluid flow over a stretchable cylinder while incorporating unsteadiness, magnetic field, and heat generation. The current study's specific goals are to: formulate an unsteady two-dimensional partial differential equations of an incompressible Carreau fluid flow; use similarity transformations to convert the equations to ordinary differential equations; use the shooting technique to numerically analyze the transformed equations via Runge-Kutta fourth order, which will be implemented on MAPLE 18.0 software; and ascertain the effects of some key parameters on the fluid flow's velocity and temperature profiles.

II. 2. MATHEMATICAL FORMULATION

The following are the fundamental assumptions for the flow system:

i. a horizontal stretchable cylinder is taken into consideration

ii. a strong magnetic field B_0 is applied inrdirection

iii. the horizontal axis represents the axial axis and the vertical axis is the radial axis

iv. it is assumed that the cylinder's stretching surface velocity is $U_w = U_0(x/a)$ and the ambient fluid velocity is $U_\infty = 0$

v. the cylinder's melting surface temperature is represented by T_∞, but the temperature of the surrounding fluid is assumed to be T_∞

vi. the solid surface temperature is represented by T_0

vii. c_s indicates the surface's heat capacity while the latent heat of the fluid in the melting layer is represented as λ_1

The diagrammatic form of the problem's physical description is shown in Figure 1

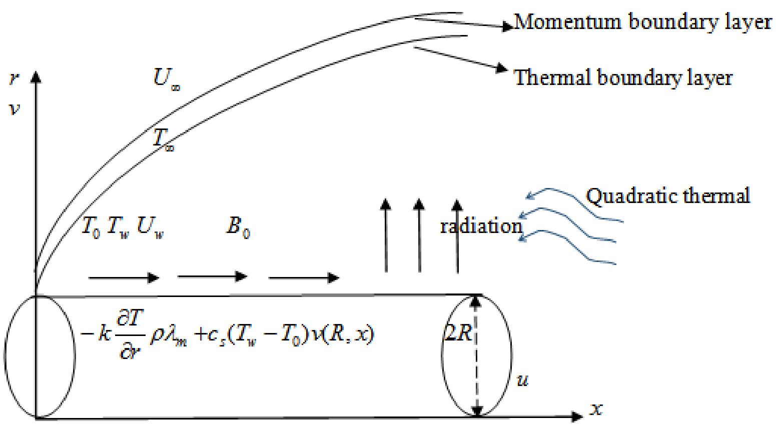

Figure 1: The problem's geometry flow (Onikolaet al. [31])

International Journal of Advances in Engineering and Management (IJAEM)
Volume 7, Issue 11 Nov. 2025, pp: 280-296 www.ijaem.net ISSN: 2395-5252

The system of governing equations for the momentum, energy and continuity equations, together with the relevant boundary conditions, is as follows: (Yeouet al.[28])

Continuity equation

$$\frac{\partial(ru)}{\partial x}+\frac{\partial(rv)}{\partial r}=0 \tag{1}$$

Momentum equation

$$\frac{\partial u}{\partial t}+u\frac{\partial u}{\partial x}+v\frac{\partial u}{\partial r}=\upsilon\left[\left(\frac{3\Gamma^2(n-1)}{2}\left(\frac{\partial u}{\partial r}\right)^2+1\right)\frac{\partial^2 u}{\partial r^2}+\frac{1}{r}\frac{\partial u}{\partial r}+\frac{\Gamma^2(n-1)}{2r}\left(\frac{\partial u}{\partial r}\right)^3\right]-\frac{\sigma B_0^2 u}{\rho} \tag{2}$$

Energy equation

$$\frac{\partial T}{\partial t}+u\frac{\partial T}{\partial x}+v\frac{\partial T}{\partial r}=\frac{1}{r}\frac{\partial}{\partial r}\left(kr\frac{\partial T}{\partial r}\right)+\frac{\partial q_r}{\partial r}+Q_0\left(T-T_\infty\right) \tag{3}$$

subject to the following boundary conditions
Momentum boundary conditions:

$$\begin{aligned}&u\to 0,\ \text{as}\ r\to\infty\\ &u=U_0a^{-1}x,\ \text{v}=0,\ \text{at}\ r=R\end{aligned} \tag{4}$$

Energy boundary conditions:

$$\begin{aligned}&k\left(\frac{\partial T}{\partial r}\right)=\rho\left[\lambda_1+c_s\left(T_w-T_0\right)\right]v(R,x),\ \ T=T_w\ \text{ at }\ r=R\\ &T\to T_\infty\ \text{ as }\ r\to\infty\end{aligned} \tag{5}$$

III. SIMILARITY TRANSFORMATION

The similarity transformation variables are used to transform equations (1) to (3) and the boundary conditions (4) and (5) into single variable differential equations.The similarity transformation variables are (Yeouet al. [28], Akl, [34], Masood et al. [35], Saima et al. [36]):

$$\eta=\sqrt{\frac{a}{\upsilon(1-\alpha t)}}\left(\frac{r^2-R^2}{2R}\right),\ \theta=\frac{\text{T - T}_\infty}{\text{T}_\text{w}-T_\infty},\quad \psi=\sqrt{\frac{\upsilon a}{(1-\alpha t)}}xRf(\eta),\ u=\frac{1}{r}\frac{\partial\psi}{\partial r},\ v=\frac{-1}{r}\frac{\partial\psi}{\partial x} \tag{6}$$

The radiative heat flux term in the Roseland approximation is given by

$$q_r=\frac{4\sigma^*}{3K^*}\frac{\partial T^4}{\partial r} \tag{7}$$

where k^* and σ^* are Roseland mean absorption coefficient and stefan Boltzman constant respectively. Using the Taylor series expansion, the temperature is expressed as the ambient temperature T_∞ then the series is truncated following the second-order term. For sufficiently larger temperature, the quadratic approximation is expressed as follows. (Yeouet al. [28], Thriveni and Mahanthesh [14]):

$$T^4\approx -8T_\infty^3+6T_\infty^2T^2+3T_\infty^4 \tag{8}$$

By virtue of equations (7) and (8) the energy equation (3) becomes

$$\frac{\partial T}{\partial t}+u\frac{\partial T}{\partial x}+v\frac{\partial T}{\partial r}=k\left(\frac{\partial^2 T}{\partial r^2}+\frac{1}{r}\frac{\partial T}{\partial r}\right)+\frac{4\sigma^*}{3k^*}\left(6T_\infty^2\frac{\partial^2 T^2}{\partial r^2}-8T_\infty^3\frac{\partial^2 T}{\partial r^2}\right)+Q_0\left(T-T_\infty\right) \tag{9}$$

The continuity equation (1) is satisfied by using the stream function. Substituting the transformation variables (6) into equations (2) and (9), the corresponding governing equations are reduced to

$$2We^2(n-1)(1+2\lambda\eta)\lambda(f'')^3+\frac{3}{2}We^2(n-1)(1+2\lambda\eta)^2(f'')^2 f'''+(1+2\lambda\eta)f'''-(f')^2$$
$$+(2\lambda+f)f''-(M+A)f'-A\frac{\eta}{2}f''=0 \tag{10}$$

$$2\lambda\theta'+\Pr f\theta'+(1+2\lambda\eta)\theta''+\frac{4}{3}Rd(1+2\lambda\eta)\theta''+\frac{12}{3}Rd(1+2\lambda\eta)(\theta_w-1)\theta'^2$$
$$+\frac{12}{3}Rd(1+2\lambda\eta)(\theta_w-1)\theta\theta''+\frac{4}{3}Rd\lambda\theta'+\frac{12}{3}Rd\lambda(\theta_w-1)\theta\theta'+\delta\theta-A\frac{\eta}{2}\Pr\theta'=0 \tag{11}$$

subject to the transformed boundary conditions

$$Me\theta'(0)+\Pr f(0)=0,\theta(0)=1$$
$$\theta(\infty)=0,\ f'(0)=1,\ f'(\infty)=0 \tag{12}$$

In the above expressions, prime indicates differentiation with respect to η, Me denotes the melting parameter, A denotes unsteadiness parameter, Rd denotes radiation parameter, $\Pr$ is the Prandl number, λ is the curvature parameter, We is the Weissenberg number, and δ denotes the heat generation parameter. These parameters are defined as (Yeouet al. [28], Akl, [34], Masood et al. [35]):

$$A=\frac{\alpha}{a},\quad M=\frac{\sigma B_0^2}{\rho U_0 a},Rd=\frac{4\sigma^* T_\infty^3}{k^* k},\quad \delta=\frac{\upsilon a Q_0}{kU_0},\quad \theta_w=\frac{T_w}{T_\infty},\quad We^2=\frac{\Gamma^2 x^2 U_0^3}{\upsilon a^3},\lambda=\frac{1}{R}\left(\frac{\upsilon a}{U_0}\right)^{1/2},$$
$$\Pr=\frac{\upsilon}{k},Me=\frac{c_p(T_\infty-T_w)}{\lambda_m+c_s(T_w-T_0)} \tag{13}$$

IV. PHYSICAL QUANTITIES

In this analysis, the physical quantities of interest are characterized by the skin friction coefficient (C_f) and the local Nusselt number (Nu) in terms of Reynold's number ($\mathrm{Re}_x^{1/2}$) which are given as (Yeouet al. [28]).

$$C_f \mathrm{Re}_x^{1/2}=2f''(0)+(n-1)We^2\{f''(0)\}^3 \tag{14}$$
$$Nu\,\mathrm{Re}_x^{-1/2}=-\left[1+\frac{4}{3}Rd+4Rd(\theta_w-1)\theta(0))\right]\theta'(0) \tag{15}$$

V. NUMERICAL PROCEDURE

Equations (10) to (12) are highly coupled and nonlinear and can't be solved analytically, hence Runge-Kutta fourth order alongside shooting technique is used to obtain numerical solutions. Applying the shooting technique, the boundary value problem is converted to initial value problem of order one by introducing new variables given as follows (Ajala et al. [13], Hashim and Ali [37]):

$$b_1=f';$$
$$b_2=b_1'; \tag{16}$$

$$b_2'=\left(\frac{2}{3We^2(n-1)(1+2\lambda\eta)^2 b_2^2+2(1+2\lambda\eta)}\right)\begin{pmatrix} b_1^2+Mb_1+Ab_1+\frac{A}{2}\eta b_2-fb_2-2\lambda b_2 \\ -2We^2(n-1)(1+2\lambda\eta)\lambda b_2^3 \end{pmatrix} \tag{17}$$

International Journal of Advances in Engineering and Management (IJAEM)
Volume 7, Issue 11 Nov. 2025, pp: 280-296 www.ijaem.net ISSN: 2395-5252

$$b_3 = \theta'; b_3' = \left(\frac{3}{3(1+2\lambda\eta) + 4Rd(1+2\lambda\eta) + 12Rd(1+2\lambda\eta)(\theta_w - 1)\theta} \right)$$

$$\left(\begin{array}{l} \frac{A}{2}\eta \Pr b_3 - \frac{4}{3}Rd\lambda b_3 - 2\lambda b_3 - \Pr\ f b_3 - \frac{12}{3}Rd(1+2\lambda\eta)(\theta_w - 1)b_3^{\ 2} \\ -\frac{12}{3}Rd\lambda(\theta_w - 1)\theta b_3 - \delta\theta \end{array} \right) \tag{18}$$

subject to the initial conditions

$$\begin{array}{l} Mer(0) + \Pr\ f(0) = 0, \theta(0) = 1 \\ p(0) = 1, q(0) = a_1, r(0) = a_2 \end{array} \tag{19}$$

The shooting technique is used to approximate the initial values a_1 and a_2 needed for the solutions to equations (16) through (19). The stated boundary conditions $f'(\eta) = 0$ and $\theta(\eta) = 0$ are compared to the corresponding results when $\eta = 10$ and the approximate values of a_1 and a_2 are adjusted to obtain a more efficient approximated solution.

Since infinity (∞) is a high number, it is assumed to be ten (10) in accordance with Shaw et al. [17], Yeouet al. [28]to make sure all the numerical solutions approach the asymptotic values correctly. Using MAPLE 18.0 software, the Runge-Kutta 4th order approach is used to solve the system of simultaneous equations after finding all the initial conditions. The classical fourth order Runge-Kutta method is introduced as follows:

$$y_{i+1} = y_i + \frac{h}{6}(m_1 + 2m_2 + 2m_3 + m_4) \tag{20}$$

where the coefficients m_1 to m_4 are respectively defined as

$$m_1 = f(x_i, y_i) \tag{21}$$

$$m_2 = f(x_i + \frac{h}{2}, y_i + m_1\frac{h}{2}) \tag{22}$$

$$m_3 = f(x_i + \frac{h}{2}, y_i + m_2\frac{h}{2}) \tag{23}$$

$$m_4 = f(x_i + h, y_i + m_3 h) \tag{24}$$

The step size is taken as h = 0.01 and the above proceeding is reiterated until the converged results are reached equal to the desired degree of accuracy, 10^{-5}.

VI. RESULTS AND DISCUSSIONS

During the computation, parametervalues are chosen as A=0.2, We = 0.5, λ = 0.1, θ_w = 1.3,n = 1.5, Rd = 1.3, Pr = 0.71, Me = 0.1, δ = -0.5, M = 0.5 (Ajala et al. [13], Yeouet al. [28], Akl[34], Elbashbeshyet al.[38]). Tables 1 and 2 reveals excellent agreement when the current work is compared to previous ones. The values of some parameters and the effects of raising them on the skin friction coefficient and Nusselt number are shown in Table 3. It is evident from the table that for any value of the various parameters taken into consideration, the Nusselt number ($\theta'(0)$) is negative. Negative numbers indicate that heat moves from the fluid to the solid surface because the fluid has higher temperature than the wall, Therefore, increasingPr, Rdand δ increases the magnitude of Nusselt number but increasing θ_w and Me decreases it.

International Journal of Advances in Engineering and Management (IJAEM)
Volume 7, Issue 11 Nov. 2025, pp: 280-296 www.ijaem.net ISSN: 2395-5252

Table 1: Comparison of Nusselt number ($-\theta^{'}(0)$) for two different values of Pr at n = 1with λ = θ_w = Me =We =Rd= δ = 0

Pr	Ishaket al.[39] $-\theta^{'}(0)$	Yeouet al.[28] $-\theta^{'}(0)$	Current work $-\theta^{'}(0)$
1	0.5820	0.5820	0.5820
10	2.3080	2.3080	2.3080

Also it is indicated from the table that the skin friction coefficient ($f^{''}(0)$) value is negative for every value of the various factors taken into consideration. In a physical scenario, the negative value of $f^{''}(0)$ indicates the surface exerts a drag force on the fluid as a result of the inducement of the flow by the stretching cylinder. However, increasing We reduces the magnitude of the skin friction coefficient while enhancing λ increases magnitude of the skin friction coefficient. Figure 2 reveals an increase in the magnetic field which yields a corresponding decrease in the velocity of the fluid flow. Physically, magnetic field is known to release Lorentz force which decelerates the motion of the fluid flow and that explains the reason for the behaviour of the flow.

The velocity profile is observed to increase by enhancing the curvature parameter in Figure 3. As a result of larger value of curvature parameter, the radius of the cylinder decreases which then enhances the velocity and momentum boundary layer thickness.

Table 2: Comparison of Skin friction ($f^{''}(0)$)for various values of λ at n = 1 with We= M = 0

λ	Gangadhar et al.[24] $f^{''}(0)$	Yeouet al. [28] $f^{''}(0)$	Current work $f^{''}(0)$
0.0	-1.00000	-1.00001	-1.00001
0.1	-1.03698	-1.03688	-1.03698
0.3	-1.11115	-1.11115	-1.11115
0.5	-1.18869	-1.18459	-1.18459

Table 3: Various values of Skin friction coefficient and Nusselt number for different parameters

We	λ	n	A	Rd	θ_w	Me	Pr	δ	$-f^{''}(0)$	$-\theta^{'}(0)$
0.5	0.1	1.5	0.2	1.3	1.3	0.1	0.71	-0.5	1.07802	0.36920
1.0	0.1	1.5	0.2	1.3	1.3	0.1	0.71	-0.5	0.97758	0.37048
0.5	**0.3**	1.5	0.2	1.3	1.3	0.1	0.71	-0.5	1.14612	0.38723
0.5	0.1	**1.0**	0.2	1.3	1.3	0.1	0.71	-0.5	1.13330	0.36866
0.5	0.1	1.5	**0.3**	1.3	1.3	0.1	0.71	-0.5	1.10715	0.36316
0.5	0.1	1.5	0.2	**1.6**	1.3	0.1	0.71	-0.5	1.07610	0.33644
0.5	0.1	1.5	0.2	1.3	**1.6**	0.1	0.71	-0.5	1.07399	0.30065
0.5	0.1	1.5	0.2	1.3	1.3	**0.4**	0.71	-0.5	1.14757	0.38069
0.5	0.1	1.5	0.2	1.3	1.3	0.1	**1.0**	-0.5	1.07237	0.38432
0.5	0.1	1.5	0.2	1.3	1.3	0.1	0.71	**-1.0**	1.08565	0.49842

International Journal of Advances in Engineering and Management (IJAEM)
Volume 7, Issue 11 Nov. 2025, pp: 280-296 www.ijaem.net ISSN: 2395-5252

Figure 4 reflects an initial decrease which switches over to increase velocity around eta = 3.0. This is because unsteadiness deforms the free stream velocity, making it unstable over a specified time. The reduction in the fluid velocity depicts that higher unsteadiness signifies more pronounced temporal fluctuations in the stretching or acceleration of the flow, which typically acts to counteract the advancement of the fluid. The effect of Weissenberg number on the velocity profile is depicted in Figure 5 which indicates that the fluid's velocity profile grows as the Weissenberg number rises. This is because a fluid that is shear thinning has less viscosity, which lowers resistance to fluid motion and raises the fluid's velocity profile.

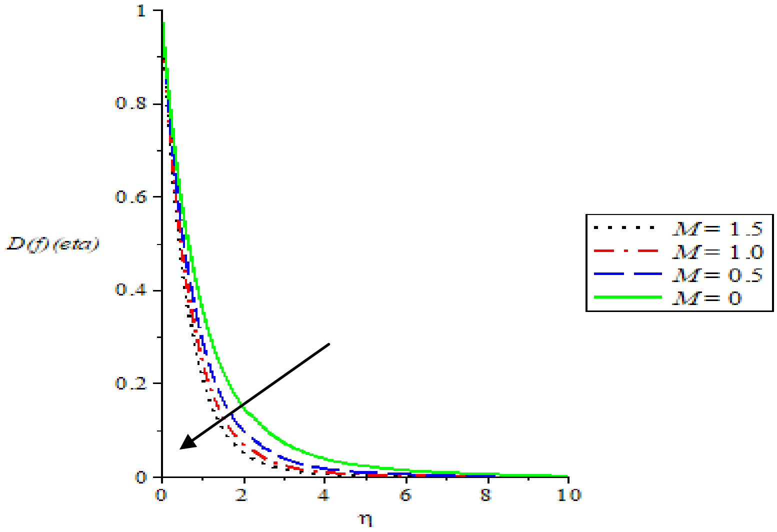

Figure 2: Impact of magnetic field parameter on the velocity profile

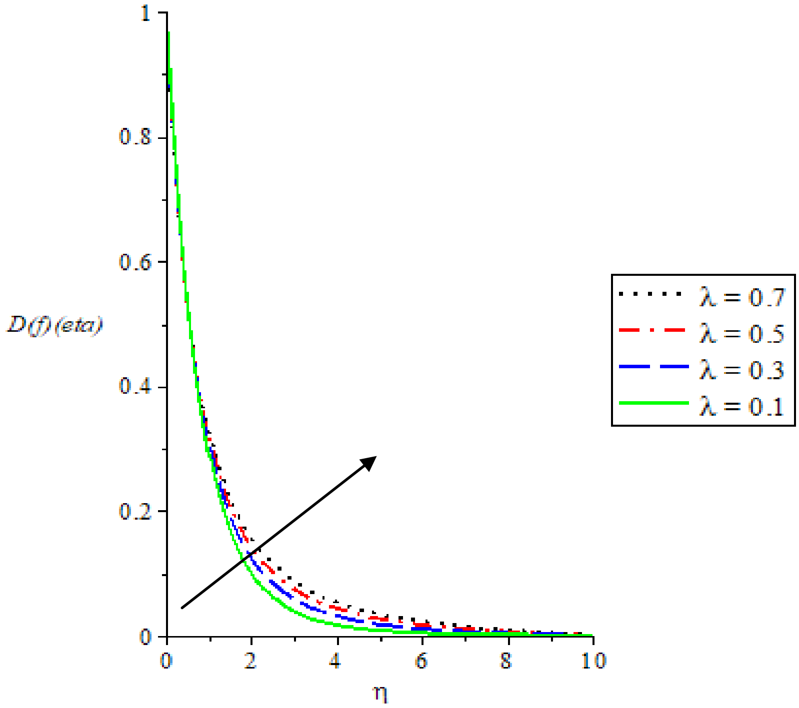

Figure 3: Impact of curvature parameter on the velocity profile

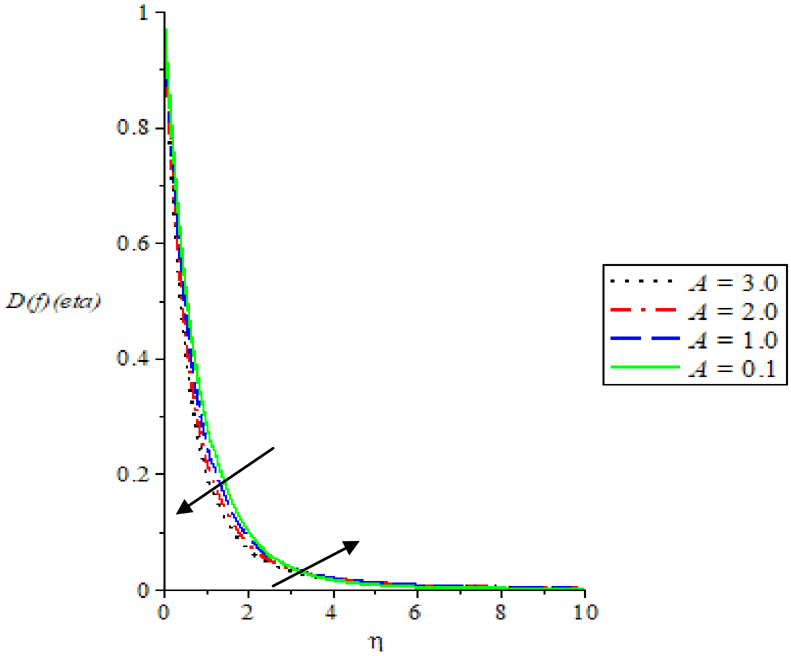

Figure 4: Impact of unsteadiness parameter on the velocity profile

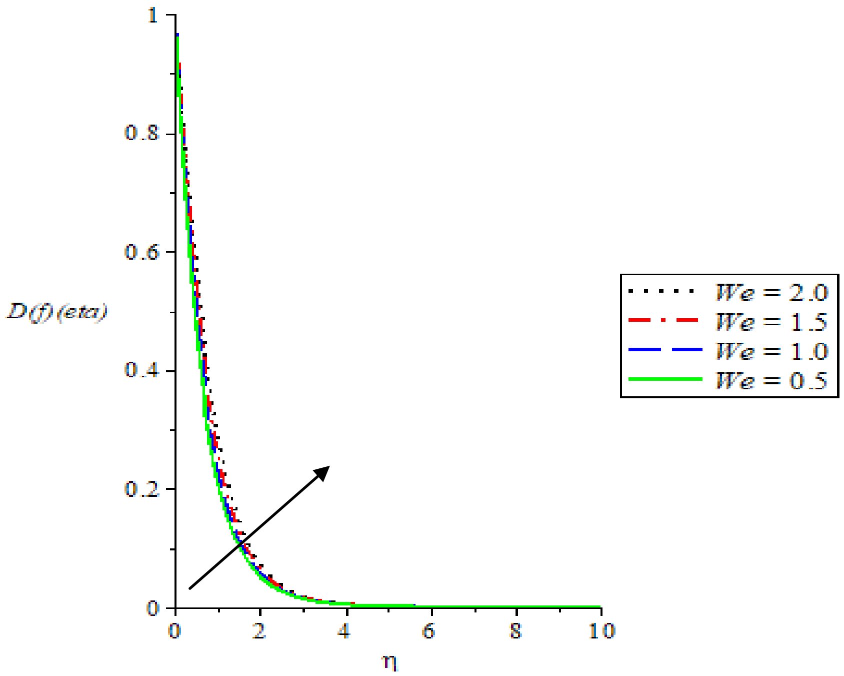

Figure 5: Impact of Weissenberg number on the velocity profile

International Journal of Advances in Engineering and Management (IJAEM)
Volume 7, Issue 11 Nov. 2025, pp: 280-296 www.ijaem.net ISSN: 2395-5252

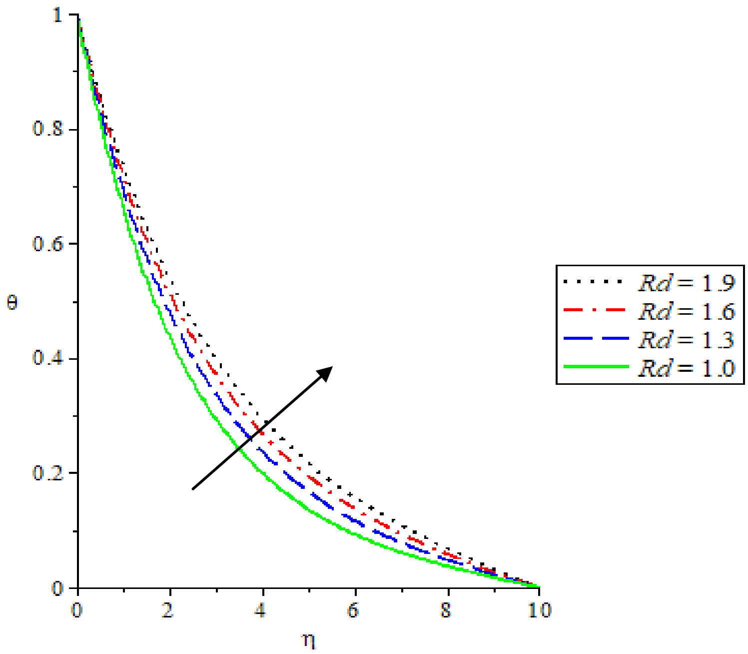

Figure 6: Impact of thermal radiation on the temperature profile

The influence of thermal radiation parameter on the temperature profile is depicted in figure 6. Increasing the thermal radiation parameter leads to an increase in flow temperature. This is because the fluid absorbs radiant energy and this absorption increases the internal energy of the fluid thereby raises its temperature.

Figure 7depicts impact of large temperature difference on the temperature profile. The flow temperature increases as the temperature ratio parameter increases.

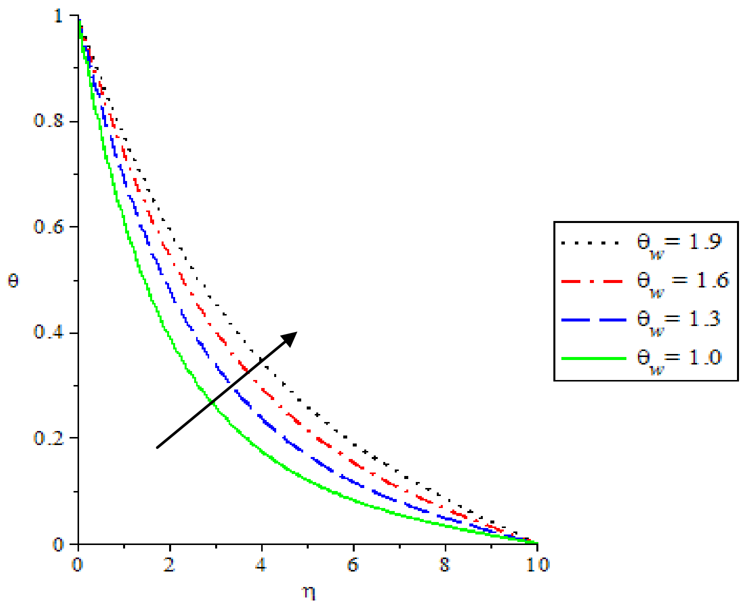

Figure 7: Impact of temperature ratio on the temperature profile

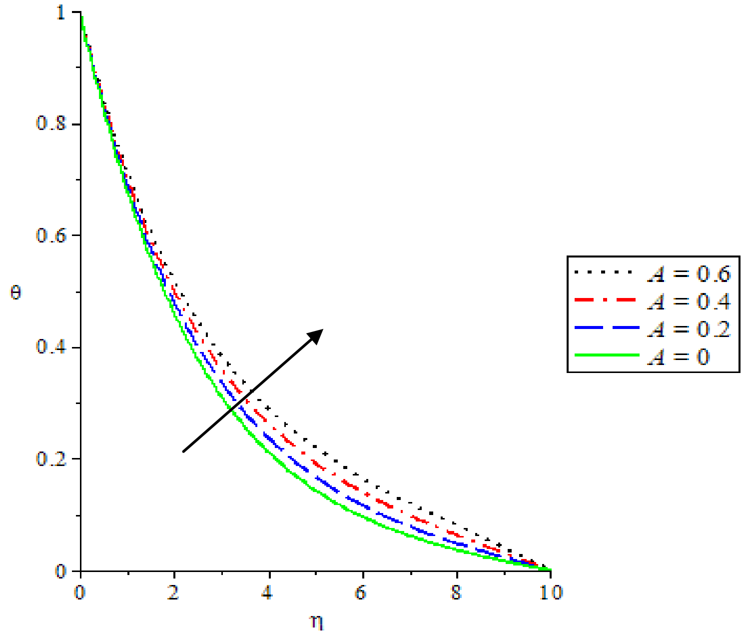

Figure 8: Impact of unsteadiness parameter on the temperature profile

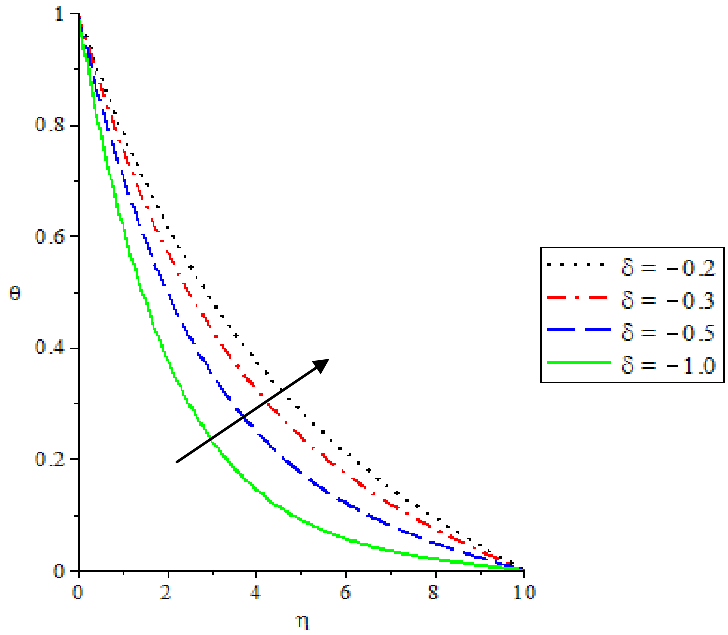

Figure 9: Impact of heat generation parameter on the temperature profile

Generally, the temperature ratio parameter enhances the heat transfer and as a result makes the fluid has a higher temperature. Figure 8 shows an increase in the temperature profile of the fluid with an increase in the unsteadiness parameter. The temperature increased as a result of the possibility of more often collision of the particles and molecules in the fluid which results in the release of heat.It is concluded from Figure 9 that an increase in heat generation parameter causes a boost in the velocity and thickness of momentum boundary layer thickness. In a physical sense, when a fluid generates heat internally, the temperature profile is altered significantly due to the addition of thermal energy within the domain.

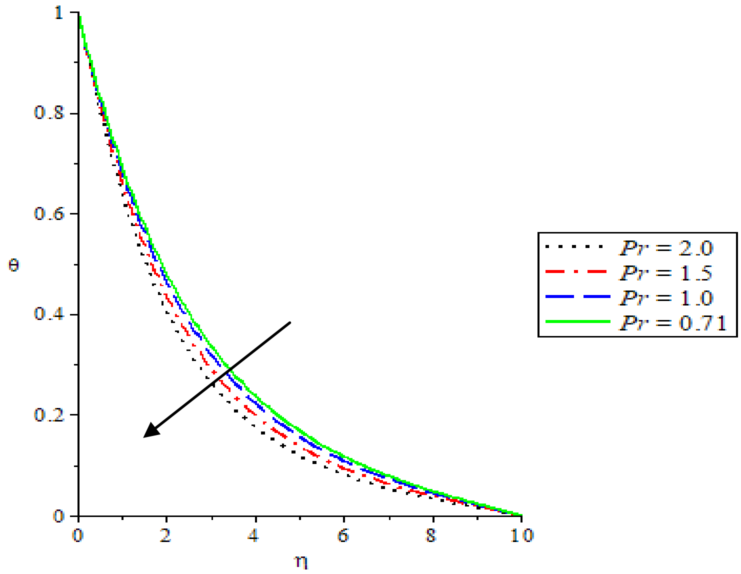

Figure 10: Impact of Prandtl number on the temperature profile

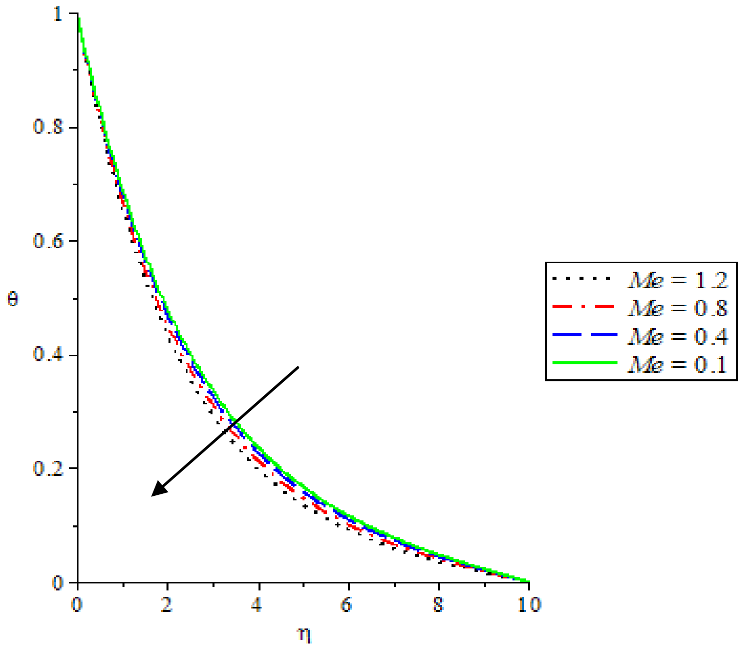

Figure 11: Impact of Melting parameter on the temperature profile

Figure 10 depicts the effect of Prandtl number on the temperature profile. Physically, higher Prandtl numbers are representatives of polymetric non-Newtonian fluids which are connected with lower thermal diffusivity. However, it is illustrated from the figure that an increase in Prandtl number reduces the temperature profile. The effect of melting parameter on the temperature profile is depicted in Figure 11. As the melting parameter increases,the flow temperature profile of the fluid decreases. This is because melting absorbs more thermal energy as more heat goes into phase change.

VII. CONCLUSION

Runge-Kutta fourth order method alongside shooting technique implemented on Maple 18.0 software was used to present the numerical solutions for the unsteady two-dimensional boundary layer flow of an incompressible Carreau fluid along a stretching cylinder. The behaviour of the fluid flow emerging parameters was investigated with respect to velocity and temperature distribution profiles. The important findings are given as follows:

- Unsteadiness, heat generation, thermal radiation and temperature ratio parameters all collaborated to strengthen the fluid temperature due to large temperature difference.
- A deteriorating thermal boundary layer thickness was spotted with a rise in the Prandtl number and melting parameter.
- A reflectionof an initial decrease which switched over to increase velocity around eta = 3.0as a result of the deformation of the free stream velocity with an enhanced unsteadiness parameter.
- There was a downturn of the momentum boundary layer of the fluid with an increase in the magnetic field parameter due to the Lorentz force released to produce substantial control of the flow. While the fluid velocity was enhanced with a boost in the curvature parameter and Weissenberg number.
- The unsteadiness parameter reduced the two physical quantities, skin friction and Nusselt number.

The findings drawn from this analysis are applicable in many areas, including heat exchangers in electronics, space cooling, power generation, magnetic drug targeting and automotive engineering. This study can be extended by considering the behaviour of more flow parameters in the presence of nonlinear thermal radiation.

REFERENCES

[1]. Osama, M. E. (2024). Introduction and Mathematical Analysis in Basics of Heat Transfer. Department of Mechanical Engineering, College of Engineering and Technology, Nile Valley University, Atbara Sudan, 1-16.https://doi.org/10.13140/RG.2.2.25235.90406

[2]. Gnaneswara, R. M., (2021). Analysis of modified Fourier law and melting heat transfer in a flow involving carbon nanotubes, Journal of Process Mechanical Engineering,**235**(5), 1259-1268.https://doi.org/10.1177/09544089211001353

[3]. Imran, M., Zaheer, A., Mahnoor, N., and Nadeem, S. (2021). Impact of Joule heating and melting on time-dependent flow of nanoparticles due to an oscillatory stretchable curved wall. Alexandria Engineering Journal, **60**(4), 4097-4113.https://doi.org/10.1016/j.aej.2021.02.055

[4]. Singh, K., Pandey, A. K., and Kumar, M. (2021). Numerical solution of micropolar fluid flow via stretchable surface with chemical reaction and melting heat transfer using Keller Box method. Propulsion and Power Research, **10**(2), 194-207.https://doi.org/10.1016/j.jppr.2020.11.006

[5]. Muhammad, K., Hayat T., and Alsaedi, A. (2021). Numerical study for melting heat in dissipative flow of hybrid nanofluid over a variable thicked surface. International Communications in Heat and Mass Transfer, **121**, 104805.https://doi.org/10.1016/j.icheatmasstransfer.2020.104805

[6]. Khan, S. A (2021). Melting heat transportation in radiative flow of nanomaterials with irreversibility analysis. Renewable and Sustainable Energy Reviews, **140**, 110739.https://doi.org/10.1016/j.rser.2021.110739

[7]. Gireesha, B. J., and Shankaralingappa, B. M., and Prasannakumar, B. C., and Basavarajappa, N. (2020). MHD flow and melting heat transfer of dusty Casson fluid over a stretching sheet with Cattaneo–Christov heat flux model, International journal of ambient energy, 1-9.https://doi.org/10.1080/01430750.2020.1785938

[8]. Ayub, A., (2022). Characteristics of melting heat transport of blood with time dependent cross-nanofluid model using Keller–Box and BVP4C method.

Engineering with Computers, **38**(4), 3705-3719.https://doi.org/10.1007/s00366-021-01406-7

[9]. Jawad, M., Ziad, K., Ebenezer, B., and Rashid, J. (2022). Analysis of hybrid nanofluid stagnation point flow over a stretching surface with melting heat transfer. Mathematical Problems in Engineering, **20**(22), 9469164.https://doi.org/10.1155/2022/9469164

[10]. Warke, A. S., Ramesh, K., Mebarek, O. F., Abidi, A. (2021). Numerical investigation of the stagnation point flow of radiative magnetomicropolar liquid past a heated porous stretching sheet. Journal of thermal analysis and calorimetry, **147**(4), 6901-6912.https://doi.org/10.1007/s10973-021-10976-z

[11]. Ajala, O, Adegbite, P., Abimbade, S. F., and Obalalu, A. M. (2019). Thermal radiation and convective heating on hydromagnetic boundary layer flow of nanofluid past a permeable stretching surface. International Journal of Applied Mathematics and Statistical Sciences, **8**(2), 43-58.https://www.researchgate.net/publication/335992388

[12]. Thriveni, K., and Mahanthesh, B. (2021). Heat transport of hybrid nanomaterial in an annulus with quadratic Boussinesq approximation. Applied Mathematics and Mechanics, **42**(6), 885-900.https://doi.org/10.1007/s10483-021-2739-6

[13]. Ajala, O. A, Adegbite, P., Obalalu, A. M., Abbas, A., Owolabi, A. O., Ojewola, O. B. (2024). Bio-Convective Flow of Micropolar Nanofluids over an Inclined Permeable Stretching Surface with Radiative Activation Energy. Journal of Biomimetics, Biomaterials and Biomedical Engineering, **65**, 1-13.https://doi.org/10.4028/p-c79R3Y

[14]. Thriveni, K., and Mahanthesh, B. (2020). Optimization and sensitivity analysis of heat transport of hybrid nanoliquid in an annulus with quadratic Boussinesq approximation and quadratic thermal radiation. European Physics Journal, **135**(6), 1–22.https://doi.org/10.1140/epjp/s13360-020-00484-8

[15]. Algehyne, E. A., (2022). Mixed convective flow of Casson and Oldroyd-B fluids through a stratified stretching sheet with nonlinear thermal radiation and chemical reaction. Journal of Taibah University for Science, **16**(1), 193-203.https://doi.org/10.1080/16583655.2022.2040281

[16]. Patil, P., and Goudar, B. (2022). Entropy generation analysis from the time-dependent quadratic combined convective flow with multiple diffusions and nonlinear thermal radiation. Chinese Journal of Chemical Engineering, **53**(1), 46-55.https://doi.org/10.1016/j.cjche.2022.01.013

[17]. Shaw, S., Samantaray, S. S., Misra, A., Manoj, K. N., and Makinde, O. D. (2022). Hydromagnetic flow and thermal interpretations of Cross hybrid nanofluid influenced by linear, nonlinear and quadratic thermal radiations for any Prandtl number. International Communications in Heat and Mass Transfer, **130**, 105816.https://doi.org/10.1016/j.icheatmasstransfer.2021.105816

[18]. Carreau, P. J. (1972). Rheological Equations from Molecular Network Theories. Journal of Rheology, **116**, 99-127.https://doi.org/10.1122/1.549276

[19]. Santoshi, P. N., Ramana, G. V., and Padma, P., (2020). Numerical scrutinization of three dimensional Casson-Carreau nanofluid flow. Journal of Applied and Computational Mechanics, **6**(2), 531-542.https://doi.org/10.22055/JACM.2019.29377.1593

[20]. Mahdy, A., Fekry, M. H., Ramadan, A. M., and Omima, A. A. (2021). Activation energy effectiveness in dusty Carreau fluid flow along a stretched cylinder due to nonuniform thermal conductivity property and temperature-dependent heat source/sink. Heat Transfer, **14**(7), 1-19.https://doi.org/10.1002/htj.22147

[21]. Afzal, S., Siddique, I., Jarad, F., Ali, R., Abdal, S., and Hussain, S. (2021). Significance of double diffusion for unsteady Carreau micropolar nanofluid transportation across an extending sheet with thermo-radiation and uniform heat source. Case Studies in Thermal

Engineering, **28**, 101397.https://doi.org/10.1016/j.csite.2021.101397

[22]. Fateh, M. O., Dharmaiah, G., Balamurugan, K. S., Ismail A. I., and Hemlata, S. (2023). The role of quadratic-linearly radiating heat source with Carreau nanofluid and exponential space-dependent past a cone and a wedge: A Medical Engineering Application and Renewable Energy. Journal Computational Bio-physics and Chemistry, **22**(8), 997–1011.https://doi.org/10.1142/S2737416523420073

[23]. Khan, M., and Azam, M., (2017b). Unsteady heat and mass transfer mechanisms in MHD Carreau nanofluid flow. Journal of Molecular Liquids, **225**, 554–562.https://doi.org/10.1016/j.molliq.2016.11.107

[24]. Gangadhar, K., Ramana, K. V., Makinde, O. D., and Kumar, B. R. (2018). MHD flow of a Carreau fluid past a stretching cylinder with Cattaneo-Christov heat flux using spectral relaxation method. Computational Analysis of Heat Transfer in Fluids and Solids, **387**, 91-105.https://doi.org/10.4028/www.scientific.net/ddf.387.91

[25]. Khan, M., Irfan M, Khan, W. A. and Alshomrani A. S. (2017). A new modeling for 3D Carreau fluid flow considering nonlinear thermal radiation. Results in Physics, **7**, 2692-2704.https://doi.org/10.1016/j.rinp.2017.07.024

[26]. Madhu, M., Mahanthesh, B., Shashi, N. S., Shehzad, S. A., Khan, S. U., and Gireesha, B. J. (2020). Performance of second law in Carreau fluid flow by an inclined microchannel with radiative heated convective condition, International Communications in Heat and Mass Transfer, **117**, 104761.https://doi.org/10.1016/j.icheatmasstransfer.2020.104761

[27]. Chu, Y. M., Israr U. R., Ijaz, M. K, Nadeem, S., Seifedine, K., Zahra, A., Nadeem A. (2020). Transportation of heat and mass transport in hydromagnetic stagnation point flow of Carreau nanomaterial: Dual simulations through Runge-Kutta Fehlberg technique, International Communications in Heat and Mass Transfer, 118, 0735-1933.https://doi.org/10.1016/j.icheatmasstransfer.2020.104858

[28]. Yeou, L. J., Ahmad,Q. M., Noraihan, A. R., Dennis, L. C., Nor, A. M., and Sharidan, S. (2023). Analysis of quadratic thermal radiation on Carreau fluid past a melting stretchable cylinder. Research Square, **10**(21), 203.https://doi.org/10.21203/rs.3.rs-2432448/v1

[29]. Maqbool, K., Awan, F., Ellahi, R. and Sait, S. (2024). Mixed convective heat and mass transfer of Carreau fluid flow past over a permeable stretching disk: thermal and concentration analysis. Journal of Thermal Analysis and Calorimetry. **150**(3).https://doi.org/10.1007/s10973-024-13696-2

[30]. Lim, Y. J., Ahmad, Q. M., Noraihan, A. R., Dennis, Ling, C. C., Nor, Athirah, M. Z., and Sharidan, S. (2024). Thermal analysis of melting effect on Carreau fluid flow around a stretchable cylinder with quadratic radiation. Propulsion and Power Research, **13**(1), 132-143.https://doi:10.1016/j.jppr.2024.02.006

[31]. Onikola, I. O., Ajala, O. A., Adegbite, P., Waheed, A. A., Akindele, A. O., and Obalalu, A. M. (2025). Magnetohydrodynamic Flow of Carreau Fluid over a Stretching Cylinder with Quadratic Thermal Radiation and Heat Generation. Adeleke University Journal of Science**4(**1), 2814-0427.https://aujs.adelekeuniversity.edu.ng/index.php/aujs/article/view/258/157

[32]. Sarma, A. K., Sarma, D., and Mudoi, S. (2025). Electromagnetohydrodynamic flow and impact of Soret, Dufour, Hall current, and activation energy on Carreau fluid through a stretching cylinder. Numerical Heat Transfer Fundamentals. 1-41.https://doi.org/10.1080/10407790.2025.2528932

[33]. Song, Y. Q. (2022). Aspects of thermal diffusivity and melting phenomenon in Carreau nanofluid flow confined by nonlinear stretching cylinder with convective Marangoni boundary constraints. Mathematics and Computers in Simulation, **195**, 138-150.https://doi.org/10.1016/j.matcom.2022.01.001

[34]. Akl, M. Y. (2014). An analytical solution for an unsteady boundary layer flow along a stretching cylinder with variable thermal conductivity. European Journal of Scientific Research. 116. 186-198.https://doi.org/10.3844/jmssp.2014.117.124

[35]. Masood, K., Muhammad, A. (2016). Unsteady boundary layer flow of Carreau fluid over a permeable stretching surface. Results in Physics, **6,** 1168-1174.https://doi.org/10.1016/j.rinp.2016.11.035

[36]. Saima, A., Imran, S., Fahd, J., Rifaqat, A., Fahd, J., and Sohaib, A. (2021). Significance of double diffusion for unsteady Carreau micropolar nanofluid transportation across an extending sheet with thermo-radiation and uniform heat source. Case Studies in Thermal Engineering. **28,**101397.https://doi.org/10.1016/j.csite.2021.101397

[37]. Hashim, M. K., and Ali, S. A. (2017). Characteristics of melting heat transfer during flow of Carreau fluid induced by a stretching cylinder. The European Physical Journal E, **40**(1), 1-9.https://doi.org/10.1140/epje/i2017-11495-6

[38]. Elbashbeshy, E. M., Emam, T. G., El-Azab, M. S., and Abdelgaber, K. M. (2012). Laminar boundary layer flow along a stretching cylinder embedded in a porous medium. International Journal of the Physical Sciences, **7**(24), 3067-3072.https://doi.org/10.5897/IJPS12.093

[39]. Ishak, A., and Nazar, R. (2009). Laminar boundary layer flow along a stretching cylinder. European Journal of ScienceResearch, **36**(1), 22-29.https://scispace.com/papers/laminar-boundary-layer-flow-along-a-stretching-cylinder-53j06as21i